

Low-Threshold Surface-Passivated Photonic Crystal Nanocavity Laser

Dirk Englund* and Jelena Vučković
Ginzton Laboratory, Stanford University, Stanford CA 94305

Hatice Altug†

Electrical and Computer Engineering Department, Boston University, Boston MA 02215
(Dated: Jan 29, 2007)

We passivate the surface of the InGaAs quantum well gain medium and GaAs membrane in a high-speed photonic crystal nanocavity laser through a (NH₄)S treatment. The passivated laser shows a five-fold reduction in surface recombination loss, resulting in a four-fold reduction in the laser threshold. A three-level laser model explains the results well and shows that for this material system, surface recombination losses are as important as cavity quality factor (Q) in determining the lasing threshold. Surface passivation therefore appears vital in operating such lasers under practical conditions.

PACS numbers:

Photonic crystals (PCs) allow unprecedented control over the radiative properties of emitters embedded inside them. High- Q cavities defined in PCs confine photons to a small volume, enabling large light-matter interaction. This property has opened new possibilities in fields including quantum electrodynamics, detection, and light sources [1, 2, 3, 4, 5, 6]. Lasers in particular stand to gain considerably through far decreased lasing threshold, modulation rate, cost, and large-scale device integration.

From the first demonstration of a PC laser [1], quantum wells (QWs) have been the most commonly used gain medium. However, in many materials such lasers are plagued by large nonradiative surface recombination losses. This problem is most salient in PC structures where the QWs expose a far greater surface area than in other types of QW lasers. Here we address the problem of QW surface recombination by surface passivation of PC laser structures. We show that surface passivation lowers the nonradiative recombination rate more than five times and observe a four-fold reduction in the lasing threshold. This increased efficiency alleviates heating problems and allows pulsed lasing at room temperature[7]. A three-level rate equations model fits our experimental data well and suggests that surface passivation is crucial for InGaAs-QW PC lasers.

The PC nanocavity lasers consist of 172 nm-thick GaAs slabs patterned with 9x9 arrays of single-hole cavities defined in a square-lattice PC (see [6]). A central stack of four 8-nm In_{0.2}Ga_{0.8}As QWs, separated by 8-nm GaAs barriers, forms the gain medium.

This sample is passivated using a solution of 7% (NH₄)S in water, which removes contamination and oxides from the GaAs and In_{0.2}Ga_{0.8}As surfaces and caps the fresh surface with sulfur atoms [8]. Samples were cleaned in Leksol, acetone, and ethanol, then treated

with the (NH₄)S for 15 minutes at 35° C and air-dried, following a recipe laid out in ref. [9]. We then measured the radiative and nonradiative properties, as well as lasing characteristics, of the sample before and after surface passivation.

We use a three-level rate model to describe the carrier and laser dynamics. Letting N_E represent the pump level carrier concentration (populated by the above-GaAs-bandgap pump laser with power L_{in}), N_G the quantum well lasing level carrier concentration (resonant with the cavity frequency), and P the cavity photon density, we have[18]

$$\begin{aligned} \frac{dP}{dt} &= \Gamma G(N_G)P + \frac{F_{cav}N_G}{\tau_r} - \frac{P}{\tau_p} \\ \frac{dN_G}{dt} &= \frac{N_E}{\tau_{E,f}} - N_G \left(\frac{F_{cav} + F_{PC}}{\tau_r} + \frac{1}{\tau_{PC,nr}} \right) - \Gamma G(N_G)P \\ \frac{dN_E}{dt} &= \eta \frac{L_{in}}{\hbar\omega_p V_a} - N_E \left(\frac{1}{\tau_{E,r}} + \frac{1}{\tau_{E,nr}} + \frac{1}{\tau_{E,f}} \right) \end{aligned} \quad (1)$$

In the center equation, we explicitly separate the total decay rate of the lasing-level carrier density N_G into components that radiate into the cavity, into other PC modes, and nonradiatively recombine: $1/\tau_G = (F_{cav} + F_{PC})/\tau_r + 1/\tau_{PC,nr}$. Here, $F_{PC} \equiv \tau_0/\tau_{PC} \approx 0.3$ expresses spontaneous emission (SE) rate quenching inside the PC bandgap compared to the bulk QW (following simulations in [5]), while $F_{cav} = \tau_0/\tau_{cav}$ denotes the SE rate enhancement into the cavity mode.

We now estimate the unknown lifetime constants in Eqs. 1 from time-resolved photoluminescence (PL) measurements. The measurements are done with a streak camera (Hamamatsu N5716-03) on PL from the PC and bulk regions, following 3.5 ps-long excitation pulses at 780 nm at 82MHz, as shown in Fig. 1. These measurements were taken at 5 K in a liquid-helium continuous-flow cryostat, where both the unpassivated and passivated samples could be brought into lasing for comparison. Using a fit to the rate model of Eqs.1, we estimate the pump-level relaxation time $\tau_{E,f}$ at ~ 6 ps for both

*Electronic address: cvitae.org/englund/

†Authors contributed equally.

treated and untreated samples (Fig. 1(b)).

After these simplifications, we can estimate the remaining decay constants from the lifetime data in Fig.1(c). PL from the bulk QW has nearly unchanged lifetime of $\tau_{bulk} \sim 571 - 614$ ps at $10\mu\text{W}$ pump power and 5K, as shown in the comparison of untreated vs. passivated bulk PL in Fig.1(c) (a small difference is due to slightly different pump focus). In contrast, PL from the patterned region shows a sharp difference: whereas before treatment, the lifetime is only $\tau_{PC} \sim 33.8$ ps due to large non-radiative surface recombination, after treatment this lifetime is extended to $\tau_{PC} \sim 142$ ps (Fig.1(b,c)). Assuming that the non-radiative rate in the bulk semiconductor is much slower than the other decay rates, we can apply the rate model of Eq.1 to the bulk semiconductor and patterned regions (i.e., we only use the bottom two equations with P and F_{cav} set to zero). In the experiment, we pump and collect emission away from the cavity. From this, we estimate for the natural bulk SE lifetime $\tau_r \approx 654$ (605) ps and nonradiative lifetime $\tau_{PC,nr} \approx 35.5$ (188) ps in the PC before (after) passivation.

Since the PL lifetime in the bulk QW is much longer than in the patterned region, nonradiative recombination in the QW occurs predominantly at the etched QW surface. The observed change in nonradiative lifetime therefore arises from a reduction in the QW surface recombination velocity S (at low pump power where Auger is small). A simple model allows us to quantify S before and after passivation. The diffusion and recombination of the carrier concentration N_G , uncoupled to the PC cavity, are described by the equation (following [10])

$$\frac{\partial N_G}{\partial t} = D\nabla^2 N_G - N_G \frac{F_{PC}}{\tau_r}, \quad (2)$$

where D is the ambipolar diffusion coefficient. Surface recombination enters through the boundary condition $D\frac{\partial N_G}{\partial r} + SN_G = 0$. Assuming isotropic minority-carrier diffusion over the period $a = 315$ nm of the photonic crystal, the total recombination rate of the PC with air holes of radius r is equivalent to that of mesas with radius r , which have equal surface area. Then Eq.2 is easily solved in cylindrical coordinates, giving the total recombination rate $1/\tau_{PC} = F_{PC}/\tau_r + 1/\tau_{PC,nr} = F_{PC}/\tau_r + 2S/r$, i.e., $\tau_{PC,nr} = r/2S$ [10]. As the hole radius r does not shrink significantly in the passivation process, we find that $S \approx 1.7 \cdot 10^5$ cm/s ($3.2 \cdot 10^4$ cm/s) for the original (passivated) structure. This value for the surface recombination velocity compares somewhat lower to previous room-temperature measurements on similar InGaAs/GaAs structures by [11, 12], which put it at between $\sim 1 \cdot 10^5$ and $5 \cdot 10^6$ cm/s. This is expected, since $S \propto v_{th} \approx \sqrt{3kT/m^*}$, the thermal velocity, which is $\sim 8\times$ smaller at 5K [13]. Our observation of a five-fold lowering in S with surface passivation is similar to other reports with $(\text{NH}_4)\text{S}$ [14]. It is likely that better passivation could be achieved with $(\text{NH}_4)\text{S}_x$, $x > 1$, for which up to $50\times$ improvement was reported [11].

With this understanding of the carrier dynamics in the

photonic crystal, we now consider the coupled cavity array laser. Microscope images show that only 7-9 cavities simultaneously lase in a single mode as fabrication inaccuracies lifted the cavity resonance degeneracies in the array. The passivation treatment slightly blue-shifts the cavity resonance and raises Q by $\sim 1.5\times$ due to cleaning and thinning of the membrane (Fig.2,c), as observed in digital cavity etching [15]. The figure also shows the passivated structure when pumped two times above threshold; here, Q is raised to 2670 due to positive gain. We estimate the average SE enhancement factor F_{cav} of emission coupled to the PC cavity from a lifetime measurement of the cold (non-lasing) cavity, giving $\tau_{cav} \approx 17$ ps. The relation for the cavity-coupled SE rate,

$$\frac{1}{\tau_{cav}} = \frac{F_{cav} + F_{PC}}{\tau_r} + \frac{1}{\tau_{PC,nr}}, \quad (3)$$

gives $F_{cav} \approx 31$.

The marked reduction in the nonradiative loss rate results in a four-fold reduction in lasing threshold (Fig.2,a). Here we compare lasing at low temperature (5 K) with pulsed (3.5 ps, 13 ns repetition) excitation, conditions under which both the original and passivated structures could be brought to lasing.

This reduction in the pump power L_{in} follows from Eqs. 1: for threshold, we solve Eqs. 1 in steady-state with $PV_{mode} = 1$ (an average of one photon inside the cavity) and $N_G \rightarrow N_{tr}$, the transparency carrier concentration. Neglecting the slow pump-level radiative recombination $\tau_{E,r}$, this gives

$$L_{in,th} = \frac{\hbar\omega_p}{\tau_p\eta} \frac{V_a}{V_{mode}} \left[N_{tr}V_{mode} \left(F_{PC} \frac{\tau_p}{\tau_r} + \frac{\tau_p}{\tau_{nr}} \right) + 1 \right] \left(1 + \frac{\tau_{E,f}}{\tau_{E,nr}} \right) \quad (4)$$

For typical parameters, $N_{tr} \approx 10^{18}$ cm $^{-3}$ [16] and $V_{mode} \approx 6(\lambda/n)^3$, the first term in the brackets $\gg 1$ and dominates. Within this term, the non-radiative part $\propto 1/\tau_{nr}$ dominates radiative one $\propto 1/\tau_r$. Thus, in PC lasers using InGaAs QWs, or other gain media with similar surface recombination velocity, we see that threshold is determined in large part by surface recombination losses at the QW and GaAs. After passivation, Eq.4 then predicts a threshold reduction to 0.20 of the original value if $\tau_{E,nr}$ is assumed much larger than $\tau_{E,f}$, and otherwise an even larger reduction. We measured a decrease by factor 3.7, which is close to the five-fold reduction that assumes $\tau_{E,nr}$ is long. The differential quantum efficiency, on the other hand, is unaffected by the nonradiative recombination rate, as can be easily derived from the rate equations (the physical reason is that once lasing begins, the stimulated emission rate is much faster than the nonradiative loss rate.)

One of the most remarkable aspects of the PC nanocavity laser is the extremely fast modulation rate. In Fig.2(b), we present streak camera measurements of the lasing response to 3.4-ps-long pump pulses. The low-temperature measurements for the passivated and unpassivated samples were obtained at the same average

pump power of $\sim 28 \mu\text{W}$ (3.5 ps, 13 ns repetition); the normalized lasing response is compared in the red and blue plots. After passivation, the laser responds somewhat faster with an exponential decay time of 6.1 ps, because it is now pumped relatively higher above threshold (due to lower nonradiative loss and higher cavity Q). Faster time response is possible at higher pump power, as noted in [6]. The model (Eqs.1) explains these measurements well.

In conclusion, we have demonstrated the threshold-lowering effect of InGaAs QW surface passivation in a PC nanocavity laser. The 5-fold reduction of nonradiative surface recombination lowers the threshold pump power to 27% of its original value. The laser response

time is improved slightly for the same power; under low-power excitation, we observed a lasing response with 6.1-ps-decay following a 3.4-ps-long excitation pulse. Our three-level laser model agrees well with experimental observations. We emphasize that our results could be considerably improved by applying more advanced surface passivation techniques [11, 17]. The increased efficiency alleviates heating problems, which opens the door to room-temperature and CW operation[7].

The authors thank Dr. Petrovykh for his helpful comments. This work was supported by the MARCO IFC Center, NSF Grants ECS-0424080 and ECS-0421483, the MURI Center (ARO/DTO Program No.DAAD19-03-1-0199), as well as the NDSEG Fellowship (D.E.).

-
- [1] O. Painter, R. Lee, A. Scherer, A. Yariv, J. O'Brien, P. Dapkus, and I. Kim, "Two-Dimensional Photonic Band-Gap Defect Mode Laser," *Science* **284**, 1819–1821 (1999).
- [2] T. D. Happ, I. I. Tartakovskii, V. D. Kulakovskii, J.-P. Reithmaier, M. Kamp, and A. Forchel, "Enhanced light emission of $\text{In}_x\text{Ga}_{1-x}\text{As}$ quantum dots in a two-dimensional photonic-crystal defect microcavity," *Physical Review B* **66**(041303) (2002).
- [3] T. Yoshie, A. Scherer, J. Hendrickson, G. Khitrova, H. M. Gibbs, G. Rupper, C. Ell, O. B. Shchekin, and D. G. Deppe, "Vacuum Rabi splitting with a single quantum dot in a photonic crystal nanocavity," *Nature* **432**, 200–203 (2004).
- [4] P. Lodahl, A. F. van Driel, I. S. Nikolaev, A. Irman, K. Overgaag, D. Vanmaekelbergh, and W. L. Vos, "Controlling the dynamics of spontaneous emission from quantum dots by photonic crystals," *Nature* **430**(7000), 654–7 (2004).
- [5] D. Englund, D. Fattal, E. Waks, G. Solomon, B. Zhang, T. Nakaoka, Y. Arakawa, Y. Yamamoto, and J. Vučković, "Controlling the Spontaneous Emission Rate of Single Quantum Dots in a Two-Dimensional Photonic Crystal," *Physical Review Letters* **95**, 013,904 (2005).
- [6] H. Altug, D. Englund, and J. Vučković, "Ultrafast photonic crystal nanocavity laser," *Nature Physics* **2**, 484–488 (2006).
- [7] D. Englund, H. Altug, and J. Vuckovic, "Room-Temperature THz Photonic Crystal Nanocavity Array Laser," to be published (2007).
- [8] H. Oigawa, J. F. Fan, Y. Nannichi, H. Sugahara, and M. Oshima, "Universal Passivation Effect of $(\text{NH}_4)_2\text{S}_x$ Treatment on the Surface of III-V Compound Semiconductors," *Japanese Journal of Applied Physics* **30**(3), 322–325 (1991).
- [9] D. Y. Petrovykh, M. Yang, and L. Whitman, "Chemical and electronic properties of sulfur-passivated InAs surfaces," *Surface Science* **523**, 231–240 (2002).
- [10] K. Tai, T. R. Hayes, S. L. McCall, and W. T. Tsang, "Optical measurement of surface recombination in InGaAs quantum well mesa structures," *Applied Physics Letters* **53**(4), 553 (1988).
- [11] G. Beister and H. Wenzel, "Comparison of surface and bulk contributions to non-radiative currents in InGaAs/AlGaAs laser diodes," *Semiconductor Science and Technology* **19**, 494–500 (2004).
- [12] S. Y. Hu, S. W. Corzine, K.-K. Law, D. B. Young, A. C. Gossard, and L. A. Coldren, "Lateral carrier diffusion and surface recombination in InGaAs/AlGaAs quantum-well ridge-waveguide lasers," *Journal of Applied Physics* **76**(8), 4479–87 (1994).
- [13] S. M. Sze, *Physics of Semiconductor Devices*, 2nd. ed. (Wiley-Interscience, New York, 1981).
- [14] M. B. et al., "Surface recombination measurements on III-V candidate materials for nanostructure light-emitting diodes," *Journal of Applied Physics* **87**(7), 3497–3504 (2000).
- [15] K. Hennessy, A. Badolato, A. Tamboli, P. Petroff, E. Hu, M. Atature, J. Dreiser, and A. Imamoglu, "Tuning photonic crystal nanocavity modes by wet chemical digital etching," *Applied Physics Letters* **87**, 021,108–1 (2005).
- [16] L. A. Coldren and S. W. Corzine, *Diode Lasers and Photonic Integrated Circuits* (New York: Wiley, 1995).
- [17] D. Y. Petrovykh, J. P. Long, and L. J. Whitman, "Surface passivation of InAs(001) with thioacetamide," *Applied Physics Letters* **86**, 242,105 (2005).
- [18] V_a : pump active volume; ω_p : cavity angular frequency; $\tau_p = Q/\omega_p$: cavity ring-down time; $G(N)$: gain; $\Gamma \approx 0.16$: confinement factor; η : pump absorption ratio; τ_r : SE lifetime in unpatterned QW, nonradiative lifetime in PC; $\tau_{PC, nr}$: nonradiative lifetime in PC; $\tau_{E, f}$, $\tau_{E, r}$, $\tau_{E, nr}$: lifetimes of pump-level relaxation, SE, and nonradiative transitions.

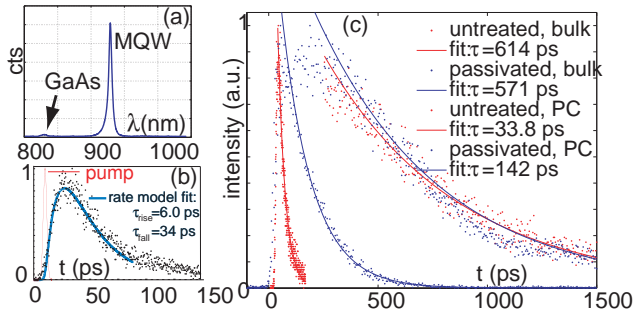


FIG. 1: Low-temperature photoluminescence measurements on unpatterned and PC regions. (a) PL from the bulk sample (after passivation). (b) Expanded view of PL from untreated PC region shows short lifetime $\tau_{PC} \approx 33.8$ ps; data is fitted by the rate model of Eqs.1. (c) PL measurements for the untreated (red) and passivated (blue) samples, from the PC and unpatterned regions.

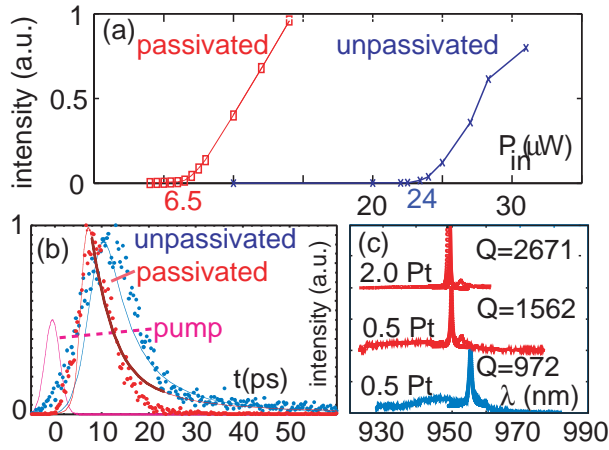


FIG. 2: LL-curves. (a) Lasing curves for unpassivated and passivated structures at low temperature (5K) with pulsed excitation (3.5 ps, 13 ns-rep.). Passivation reduces threshold from 24 μW to 6 μW (focused to a $\sim 1\mu m$ -spot). (b) Laser time response for untreated (blue) and treated (red) samples at 5K; three-level laser model of Eqs.1 fit the data reasonably well. The treated laser shows an exponential decay time of 6.1 ps (thick fit). Some deviations at longer times are caused by background PL from regions not coupled to the cavity. (c) Cavity resonances below and above lasing. Passivation lowers the resonance wavelength and slightly increases Q , as seen in the untreated (blue) and treated (red) cold-cavity spectra. Top spectrum (red): lasing of passivated structure, pumped 2x above threshold.